Trans. Phenom. Nano Micro Scales, 2(1): 1-13, Winter - Spring 2014
DOI: 10.7508/tpnms.2014.01.001

ORIGINAL RESEARCH PAPER

Prediction of Pressure Drop of Al_2O_3-Water Nanofluid in Flat Tubes Using CFD and Artificial Neural Networks

H. Safikhani[1], A. Abbassi[1,*], S. Ghanami[2]
[1] *Department of Mechanical Engineering, Amirkabir University of Technology, Tehran, I.R. Iran*
[2] *Department of Mechanical Engineering, University of Sistan & Baluchestan, Zahedan, I.R. Iran*

ARTICLE INFO.

Article history
Received 4 August 2013
Accepted 1 November 2013

Keywords
ANN
GMDH
Mixture model
Nanofluid
Pressure drop

Abstract

In the present study, Computational Fluid Dynamics (CFD) techniques and Artificial Neural Networks (ANN) are used to predict the pressure drop value (Δp) of Al_2O_3-water nanofluid in flat tubes. Δp is predicted taking into account five input variables: tube flattening (H), inlet volumetric flow rate (Q_i), wall heat flux (q_w^n), nanoparticle volume fraction (Φ) and nanoparticle diameter (d_p). The required output data for training the ANN are taken from the results of numerical simulations. The numerical simulations of nanofluid are performed using two phase mixture model by FORTRAN programming language. The flow regime and the wall boundary conditions are assumed to be laminar and constant heat flux respectively. The ANN results are compared with the numerical simulated one and excellent agreement is observed. To view the accuracy of ANN model, statistical measures R^2, RMSE and MAPE are used and it is seen that the ANN model has high accuracy in predicting the (Δp) values.

1. Introduction

In different types of heat exchangers, pressure drop is an important objective function, which must be constantly controlled. In recent years, different and effective mechanisms have been introduced and applied to improve the heat transfer value in various types of heat exchangers and tubes. However, most of these mechanisms, in addition to increasing the heat transfer, also elevate the amount of pressure drop in tubes. The increase of heat transfer has already been researched in numerous investigations; but unfortunately, the reduction and control of pressure drop in tubes has been less studied and discussed. This paper has tried to model and evaluate, from the perspective of pressure drop control, the two mechanisms employed for the increase of heat transfer in heat exchangers i.e., the use of nanofluids and flat tubes, which have already been investigated from the perspective of heat transfer increase in various research works. In this paper, the pressure drop of Al_2O_3-water nanofluid in horizontal flat tubes will be modeled and investigated by simultaneous using of the Computational Fluid Dynamics (CFD) techniques and Artificial Neural Networks (ANN).

* Corresponding author
Email Address: abbassi@aut.ac.ira

The use of nanofluids is one of the most effective mechanisms for increasing the amount of heat transfer in tubes. Nanofluid is a mixture created from adding nanoparticles, such as Al_2O_3 or CuO to a base fluid and it gives rise to increasing the mixture thermal conductivity as well as heat transfer in tubes. In recent years, many experimental and numerical studies have been done in the field of nanofluids [1-4]. Teng et al. [3] investigated the effects of various parameters such as nanoparticle size, temperature and weight fraction on the Al_2O_3-water nanofluid thermal conductivity in a series of experimental tests. In the end, they proposed a correlation indicating the nanofluid thermal conductivity as a function of mentioned parameters. In addition to the expensive experimental studies, numerical ones are considered as the effective way to identify the thermal and hydrodynamics flow field in nanofluids. In general, for numerical simulation of nanofluids flow, the single phase

Nomenclature

a	Acceleration (m s^{-2})
C_p	Specific heat (J kg^{-1} K^{-1})
C_f	Skin friction coefficient
C	Constant in Eq. (14)
d_p	Diameter of nanoparticles (m)
g	Gravitational acceleration (m s^{-2})
H	Flat tube internal height (mm)
Gr	Grashof number ($= g\beta_m q'' D_h^4 / k_m \nu_m^2$)
k	Thermal conductivity (W m^{-1} K^{-1})
k_B	Boltzmann constant (=1.3807 $\times 10^{-23}$ J K^{-1})
L	Length of tubes (m)
Nu	Nusselt Number ($= hD_h / k$)
P	Pressure (Pa)
Pr	Prandtl number ($= \alpha_m / \nu_m$)
Q	Volumetric flow rate (m^3/ hr)
q''	Heat flux (W m^{-2})
Re	Reynolds number ($= VD_h / \nu_m$)
T	Temperature (K)
V	Velocity (m s^{-1})
W	Width of flat area in tubes (mm)

Greek symbol

α	Thermal diffusivity ($= k / \rho C_p$)
β	Volumetric expansion coefficient (K^{-1})
δ	Distance between particles (m)
ϕ	Nanoparticles volume fraction
λ_f	Mean free path of water molecular (m)
μ	Dynamic viscosity (N s m^{-2})
ν	Kinematic viscosity (m^2 s^{-1})
ρ	Density (kg m^{-3})
τ_w	Wall shear stress

Subscripts

BF	Base fluid
CT	Circular tube
dr	Drift
f	Fluid
in	Inlet conditions
k	Indices
m	Mixture
p	Nanoparticle phase
w	Wall

and two phase methods are available that the two phase method is more accurate [5]. Lotfi et al. [6] investigated nanofluids flow in horizontal circular tubes with three different methods, which are single phase method, two phase mixture method and two phase Eulerian-Eulerian method. By comparison with experimental results, they found that the two phase mixture method is more accurate than the other two methods. Shariat et al. [7] used two phase mixture method to simulate the Al_2O_3-water nanofluid flow in straight elliptical tubes. They investigated laminar flow regime and mixed convection flow and discussed the effect of various parameters such as Richardson number and particle size on the thermal and

hydrodynamic flow field. One of the other methods for increasing the heat transfer in tubes is the use of flat tubes instead of circular ones. Compared to circular tubes, the flat tubes have higher surface area to cross sectional area ratio, which can be used to increase the compactness and enhance the heat transfer of the heat exchangers [8]. In the field of using flat tubes in which the nanofluids are flowing, very few studies have been conducted so far [8, 9]. Razi et al. [8] considered CuO-Oil nanofluid experimentally in various flat tubes and finally presented relations for Nusselt number and pressure drop of nanofluid flow in horizontal flat tubes. Vajjha et al. [9] investigated nanofluid flow in a single flat tube of an automobile radiator using the single phase numerical method. They used convection heat transfer coefficient for the wall boundary condition and finally presented the correlation for local Nusselt number and friction factor of the automobile flat tube. Experimental and numerical studies of nanofluids are very expensive and time consuming, hence the ANN modeling can be replaced for prediction of thermal and hydrodynamic field of nanofluids. One of the most complete and extensively used ANN types is the Grouped Method of Data Handling (GMDH). In fact GMDH is a useful tool that can convert experimental and numerical discrete data into continuous functions. The main aim of GMDH modeling is to create a quadratic polynomial function in a feed forward network whose coefficients can be obtained using regression method [10]. In recent years, many researchers have applied neural networks and GMDH for modeling of various parameters in engineering issues [11-13]. In this paper, GMDH type of ANN is used to predict the pressure drop (Δp) of Al_2O_3-water nanofluid in horizontal flat tubes taking into account five input variables: tube flattening (H), inlet volumetric flow rate (Q_i), wall heat flux (q_w^n), nanoparticle volume fraction (Φ) and nanoparticle diameter (d_p). The required output data for training the ANN are taken from the results of numerical simulations.

2. Defining the input variables

In the present study there are five independent input variables: tube flattening (H), inlet volumetric flow rate (Q_i), wall heat flux (q_w^n), nanoparticle volume fraction (Φ) and nanoparticle diameter (d_p). The variation range of each one is shown in Table 1. As shown in this table each input variable is defined in five levels. By changing the input variables according to the Table 1, various designs will be created and simulated by CFD then, the GMDH polynomials can be generated to define the pressure drop of Al_2O_3-water nanofluid in flat horizontal tubes.

Table 1
Input variables and their range of variations

Input Variables	From	To	Selected values
$H\,(mm)$	2	10	2, 4, 6, 8, 10
$Q_i\,(m^3/hr)$	0.002826	0.014130	0.002826, 0.005652, 0.008478, 0.011304, 0.01413
$q''_w\,(kW/m^2)$	1	5	1, 2, 3, 4, 5
$\phi\,(\%)$	0	5	0, 1.25, 2.5, 3.75, 5
$d_P\,(nm)$	20	100	20, 40, 60, 80, 100

According to H and Qi values of Table 1, the Reynolds number varies between 100 and 500 hence, the flow regime is laminar. Moreover the five flat tubes in this paper have different flattening and the same perimeter as shown in Fig.1 The same perimeter is a constraint which is observed by the other researchers who have studied the flat tubes [14-16]. It is evident that since the perimeter of tubes are constant, the H and W parameters in Fig. 1 depend on each other and if one of them is known, the other one could be calculated with respect to the constant perimeter constraint. Therefore in this paper, "H" is used to define each flat tube.

3. Mathematical modeling

3.1. Mixture model

In the present study, numerical simulation of nanofluid flow is performed using two phase mixture model. The mixture model is a two phase numerical method that assumes local equilibrium over short spatial length scales. The two phases are treated to be interpenetrating continua, meaning that each phase has its own velocity vector field, and within a given control volume there is a certain fraction of each phase. Instead of utilizing the governing equations of each phase separately, it solves the continuity, momentum and energy equations for the mixture, and the volume fraction equation for the secondary

phases, as well as algebraic expressions for the relative velocities. The equations for the steady state conditions and mean flow are:

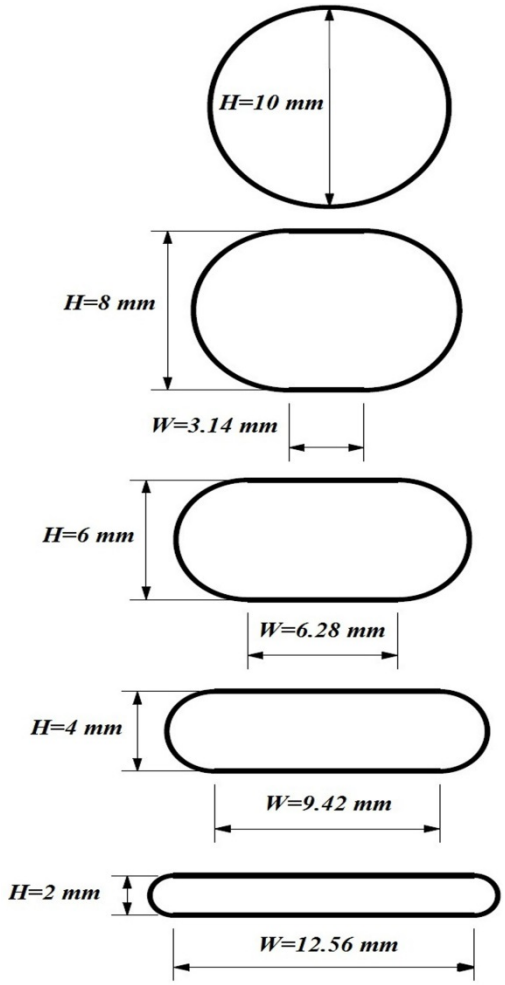


Fig. 1. Dimensions of five flat tube cross sections in the present simulations

Continuity Equation:

$$\nabla.(\rho_m V_m) = 0 \tag{1}$$

• Momentum equation:

$$\nabla.(\rho_m V_m V_m) = -\nabla P + \nabla.(\mu_m \nabla V_m) + \nabla.(\sum_{k=1}^{n} \phi_k \rho_k V_{dr,k} V_{dr,k}) - \rho_{m,i} \beta_m g(T - T_i) \tag{2}$$

• Energy equation:

$$\nabla.(\sum_{k=1}^{n} \phi_k V_k (\rho_k H_k + P)) = \nabla.(k_m \nabla T) \tag{3}$$

• Volume fraction:

$$\nabla.(\phi_P \rho_P V_m) = -\nabla.(\phi_P \rho_P V_{dr,P}) \tag{4}$$

Where Vm is the mass average velocity:

$$V_m = \frac{\sum_{k=1}^{n} \phi_k \rho_k V_k}{\rho_m} \tag{5}$$

In Eq. (2), $V_{dr,k}$ is the drift velocity for nanoparticles:

$$V_{dr,k} = V_k - V_m \tag{6}$$

The slip velocity (relative velocity) is calculated as the velocity of nanoparticles relative to the velocity of base fluid:

$$V_{pf} = V_p - V_f \tag{7}$$

The relation between drift velocity and relative velocity is as follows:

$$V_{dr,p} = V_{pf} - \sum_{k=1}^{n} \frac{\phi_k \rho_k}{\rho_m} V_{fk} \tag{8}$$

The relative velocity and drag function are calculated using Manninen et al. [17] and Schiller and Naumann [18] relations respectively, as follows:

$$V_{pf} = \frac{\rho_P d_P^2}{18 \mu_f f_{drag}} \frac{(\rho_P - \rho_m)}{\rho_P} a \tag{9}$$

$$f_{drag} = \begin{cases} 1 + 0.15\, Re_P^{0.687} & Re_P \le 1000 \\ 0.0183\, Re_P & Re_P > 1000 \end{cases} \tag{10}$$

The acceleration (a) in Eq. (9) is

$$a = g - (V_m.\nabla)V_m \tag{11}$$

3.2. Nanofluid mixture properties

The mixture properties for Al_2O_3-water nanofluid are calculated based on following expressions:

Density [19]:

$$\rho_m = \phi\rho_p + (1-\phi)\rho_f \tag{12}$$

Specific heat capacity [20]:

$$(\rho C_p)_m = \phi(\rho C_p)_p + (1-\phi)(\rho C_p)_f \tag{13}$$

Dynamic viscosity [21]:

$$\mu_m = \mu_f + \frac{\rho_p V_B d_p^2}{72 C \delta} \tag{14}$$

Where V_B and δ are Brownian velocity of nanoparticles and distance between nanoparticles respectively and can be calculated from:

$$V_B = \frac{1}{d_p}\sqrt{\frac{18 k_B T}{\pi \rho_p d_p}} \tag{15}$$

$$\delta = \sqrt[3]{\frac{\pi}{6\phi}} d_p \tag{16}$$

C in Eq. (14) is defined as:

$$C = \frac{(C_1 d_p + C_2)\phi + (C_3 d_p + C_4)}{\mu_f} \tag{17}$$

Where C1, C2, C3 and C4 are given as:

$$C_1 = -0.0000011 \; C_2 = -0.0000027$$
$$C_3 = 0.00000009 \; C_4 = -0.0000003 \tag{18}$$

Thermal conductivity [22]:

$$\frac{k_m}{k_f} = 1 + 64.7\phi^{0.7460}\left(\frac{d_f}{d_p}\right)^{0.3690} \left(\frac{k_p}{k_f}\right)^{0.7476} Pr_f^{0.9955} Re_f^{1.2321} \tag{19}$$

Where Prf and Ref are defined as:

$$Pr_f = \frac{\eta}{\rho_f \alpha_f} \tag{20}$$

$$Re_f = \frac{\rho k_B T}{3\pi\eta^2 \lambda_f} \tag{21}$$

Where λ_f is mean free path of water molecular (λ_f= 0.17 nm), kB is Boltzmann constant (k_B= 1.3807 × 10-23 J/K) and η can be defined by the following equation:

$$\eta = A.10^{\frac{B}{T-C}}, A = 2.414\times10^{-5}$$
$$B = 247.8, C = 140 \tag{22}$$

Thermal expansion coefficient [23]:

$$\beta_m = \frac{\beta_p}{1+\frac{(1-\phi)\rho_f}{\phi\rho_p}} + \frac{\beta_f}{1+\frac{\phi}{1-\phi}\frac{\rho_p}{\rho_f}} \tag{23}$$

3.3. Boundary conditions

For numerical simulation, the equations of previous sections should be solved subject to the following boundary conditions:

Tubes inlet:

$$V_{m,z} = V_i, \; V_{m,x} = V_{m,y} = 0 \tag{24a}$$
$$T = T_i \tag{24b}$$
$$\phi = \phi_i \tag{24c}$$

Fluid-wall interface:

$$V_{m,x} = V_{m,y} = V_{m,z} = 0 \tag{25a}$$

$$q''_w = -k_m \left.\frac{\partial T}{\partial n}\right|_w \tag{25b}$$

Tubes outlet: Zero gradient is applied to hydrodynamic variables and constant gradient is applied to temperature [4, 24]:

$$\frac{dV_z}{dz} = 0 \tag{26a}$$

$$\frac{dT}{dz} = cte = \frac{P}{A}\frac{q''}{\rho U C_p} \tag{26b}$$

Thus the numerical procedure is reliable and can well predict the process throughout the reactor.

3.4. Numerical methods

The strategy for solving the nanofluid flow in flat tubes is as follows. All the governing equations (described in the previous sections) for the flat rectangular section are solved in the Cartesian coordinate, and the governing equations for the two semicircular sections are solved in the cylindrical coordinate; and at the interface points of the two coordinates, all the corresponding variables in the two coordinates are set equal to each other. This notion has been schematically illustrated in Fig. 2. The numerical simulation is performed using the finite volume method by FORTRAN programming language.

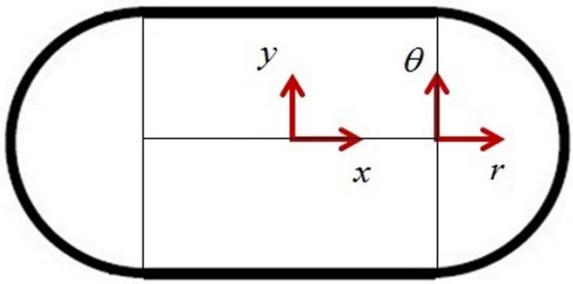


Fig. 2. Using Cartesian coordinate for rectangular flat part and cylindrical coordinate for two semicircular parts of flat tubes.

The hybrid differencing scheme is used for the convective terms and the SIMPLE algorithm is employed to solve the coupling between the velocity and pressure fields. For grid generation, first, the system boundaries are determined and then by interpolating these boundaries, the inner points are generated. For this purpose, the lower and upper boundaries have been considered as $\vec{r}_L(\zeta,\eta_{min})$ and $\vec{r}_U(\xi,\eta_{max})$, respectively. In this case, a linear one directional interpolation for finding the inner points of the field is defined as follows:

$$\vec{r}(\xi,\eta) = (1-\overline{\eta})\vec{r}_L(\zeta,\eta_{min}) + \overline{\eta}\vec{r}_U(\xi,\eta_{max}) \tag{27}$$

$$\overline{\eta} = (\eta-\eta_{min})/(\eta_{max}-\eta_{min}) \tag{28}$$

In the generated grid, because of the large hydrodynamic and thermal gradients, an exponential function is used near the walls and also at the tube inlet. This function is expressed as:

$$f(\overline{\eta}) = 1+\omega\left(\frac{1-\alpha^{(1-\eta)}}{1+\alpha^{(1-\eta)}}\right) \qquad \alpha = \frac{\omega+1}{\omega-1} \tag{29}$$

Where, ω is the clustering ratio. To implement the above functions, four line segments are considered in each tube, and the number of points specified on these four line segments determines the form of the generated grid for each flat tube. As shown in Fig. 3, these numbers of points have been designated by G_1, G_2, G_3 and G_4, and they respectively indicate the number of points along the width of the flat part, length of the flat section, perimeter of the semi circles and along the length of the tube.

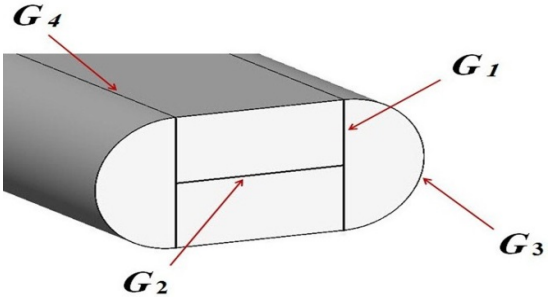


Fig. 3. Number of grid in different parts of flat tubes in grid generation step.

Fig. 4 shows a generated grid for a flat tube using the mentioned method.

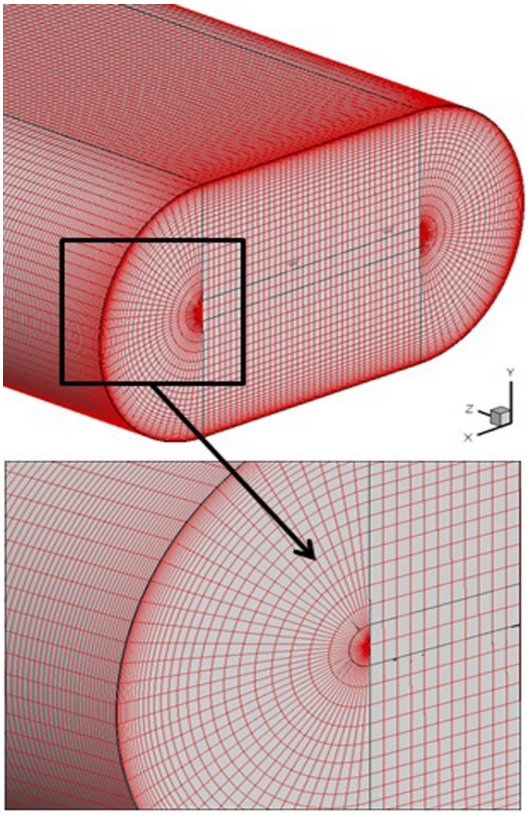


Fig. 4. Grid generation for the flat tube with H=6 mm as an example of structured non-uniform grid generations for flat tubes.

operating conditions which are used in the CFD simulations are shown in Table 2.

Table 2
Dimensions and some operating conditions for CFD simulations

Parameter	Value
Tube lengths (mm)	1000
Tube perimeters (mm)	31.4
Water density (kg/m3)	998.2
Al_2O_3 density (kg/m3)	3720
Water thermal conductivity (W/m K)	0.6028
Al_2O_3 thermal conductivity (W/m K)	35
Inlet temperature (K)	300

3.5. Validations of the numerical simulations

To attain the confidence about the CFD results, it is necessary to compare the simulation results with the available data. Fig. 5 compares the and versus flattening, predicted in the present study with analytical data of Shah and London [26] and numerical simulations of Vajjha et al. [9]. The simulations of Vajjha et al. [9] are performed for specified convection coefficient wall boundary condition whereas present simulations and Shah and London [26] data are related to constant heat flux wall boundary condition. As evident from Fig. 5 the present CFD simulations agree well with the available numerical and analytical data.

For more validations when the working fluid is nanofluid, Fig.6 is presented. This figure compares the local heat transfer coefficient and the local skin friction coefficient for a circular tube (case H=10 mm in the present study) of present study and the numerical study carried out by Mirmasoumi and Behzadmehr [27] and Shariat et al. [7]. As shown good agreement between the present simulation results and the reported numerical one are observed, hence the CFD simulations can be used for data base generation of GMDH modeling in the next section.

4. Modeling of using GMDH type ANNs

The GMDH type neural network is one of the most complete and extensively used neural networks that exist today. In this method, the neurons of the neural network are formed by relating different pairs through a quadratic polynomial. By combining the quadratic polynomials obtained from all the neurons, the network expresses the approximation function $\hat{f}$ with output $\hat{y}$ for a set of inputs ((x=($x_1, x_2, \dots, x_n$)with the least value of error in comparison with the real output Thus, for M data including n inputs and one output, the real results are expressed as follows:

$$y_i = f(x_{i1}, x_{i2}, x_{i3}, \dots, x_{in}) \quad (i = 1,2,3,\dots,M) \tag{30}$$

In fact, we are seeking a neural network of GMDH type which can predict the value of output $\hat{y}$ for every input vector x. Hence:

$$\hat{y}_i = \hat{f}(x_{i1}, x_{i2}, x_{i3}, \dots, x_{in}) \quad (i = 1,2,3,\dots,M) \tag{31}$$

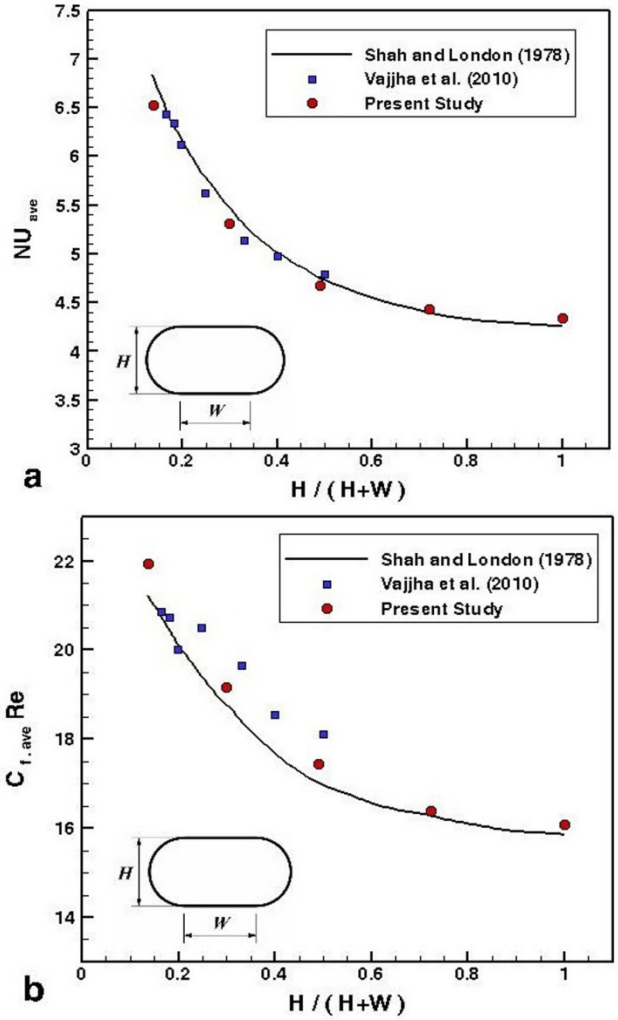
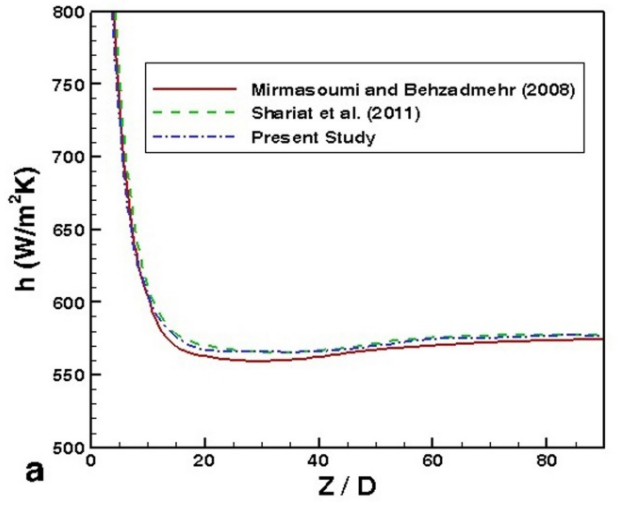


Fig. 5. Comparison of (a) and (b) of the present numerical simulation with the analytical results from Shah and London [26] and numerical results of Vajjha et al. [9] for different flat tubes at Re=100 (base fluid).



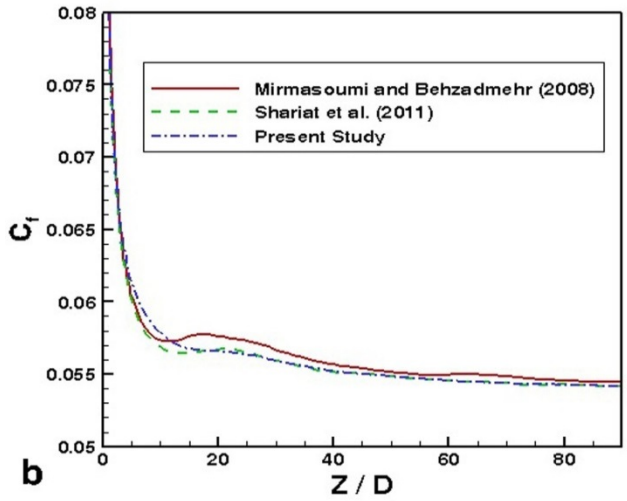


Fig. 6. Comparison of the simulation results of present study and the numerical simulations of Mirmasoumi and Behzadmehr [27] and Shariat et al. [7] for a circular tube (case H=10 mm) (a) local heat transfer coefficient (b) local skin friction coefficient (nanofluid).

The considered GMDH type neural network should be able to minimize the square of error between the real and the predicted values; in other words:

$$\sum_{i=1}^{M} [\hat{f}(x_{i1}, x_{i2}, ..., x_{in}) - y_i]^2 \rightarrow min \qquad (32)$$

The general form of relation between the input and output variables can be expressed as follows by means of a complicated polynomial function:

$$y = a_0 + \sum_{i=1}^{n} a_i x_i + \sum_{i=1}^{n}\sum_{j=1}^{n} a_{ij} x_i x_j + \sum_{i=1}^{n}\sum_{j=1}^{n}\sum_{k=1}^{n} a_{ijk} x_i x_j x_k + \qquad (33)$$

The above relation is known as Ivakhnenko polynomial [28]. In many cases, a quadratic form of this polynomial is used as follows:

$$\hat{y} = G(x_i, x_j) = a_0 + a_1 x_i + a_2 x_j + a_3 x_i x_j + a_4 x_i^2 + a_5 x_j^2 \qquad (34)$$

The GMDH is now used to find the polynomial models of heat transfer coefficient of Al_2O_3-water nanofluid flow in flat tubes with respect to their effective input parameters. In this paper, Response Surface Methodology (RSM) which is a sub method of Design of Experiments (DOE) is used [29, 30] for designing the number of input-output data in GMDH modeling. There are a total number of 52 input-output CFD data considering five input and one output variables. Samples of numerical results, using CFD are shown in Table 3. The GMDH polynomial for defining the Δp for nanofluid flows in horizontal flat tubes are obtained as:

$$Y_1 = 25.3 - 1.9H - 1.2\ q'' + 0.33\ H^2 + 0.55\ q''^2 + 0.002\ H\ q'' \quad (35a)$$

$$Y_2 = 2.61 + 2900.07\ Q_{in} - 0.105\ d_P + 49.17\ Q_{in}^{\ 2} + 0.0008\ d_P^{\ 2} + 0.153\ Q_{in}\ d_P \quad (35b)$$

$$Y_3 = 129.902 - 29.45\ \phi - 0.41\ q'' + 1.83\ \phi^2 + 0.08\ q''^2 - 0.006\ \phi q'' \quad (35c)$$

$$Y_4 = -44.34 + 4.11\ Y_1 - 0.58\ H - 0.089\ Y_1^{\ 2} + 0.0048\ H^2 + 0.055\ Y_1\ H \quad (35d)$$

$$Y_5 = 93.05 - 19.74\ Y_2 + 0.90 Y_3 + 1.28 Y_2^{\ 2} - 0.003\ Y_3^{\ 2} - 0.15\ Y_2\ Y_3 \quad (35e)$$

$$\Delta P = -2.81 + 0.31\ Y_4 - 0.04 Y_5 - 0.005\ Y_4^{\ 2} + 0.001\ Y_5^{\ 2} + 0.03\ Y_4 Y_5 \quad (35f)$$

The relationship between input and output functions has been illustrated in Fig. 7. As can be observed, in this modeling two internal layers have been used and ultimately, the pressure drop has got a structure of 'acaabdce' where a, b, c, d and e denote the values of H, Q_i, q^n , d_p and $\emptyset$, respectively. The modeling accuracy of the extracted GMDH models in predicting the CFD data has been demonstrated in Figs. 8 and 9 using two different methods. As the figures show, the ANN models predict the CFD data with very good accuracy and with an error of less than ±10%. According to Fig. 8, the 52 existing data have been divided into two groups; 40 data have been used to train, and the remaining 12 data have been used to test the network. Besides observing the prediction ability of the neural network models in Figs. 8 and 9, the capability of the models can also be evaluated through statistical means. For this purpose, three statistical parameters called the absolute fraction of variance (R_2), the Root Mean Square Error (RMSE) and the Mean Absolute Percentage of Error (MAPE) are used. These parameters are defined by the following relations:

$$R^2 = 1 - \sum_{i=1}^{n} \frac{(Y_{i\ ANN} - Y_{i\ CFD})^2}{Y_{i\ CFD}^2} \quad (36)$$

$$RMSE = \sqrt{\frac{\sum_{i=1}^{n} (Y_{i\ ANN} - Y_{i\ CFD})^2}{n}} \quad (37)$$

$$MAPE = \left(\frac{1}{n} \sum_{i=1}^{n} \frac{(Y_{i\ ANN} - Y_{i\ CFD})}{Y_{i\ CFD}}\right) \quad (38)$$

The mentioned statistical parameters have been calculated and are presented in Table 4. As observed, the statistical values also indicate the high accuracy of the obtained models in the prediction of the numerical CFD data.

5. Conclusions

In this paper GMDH type of ANN was used to predict the pressure drop value (Δp) of Al_2O_3-water nanofluid in horizontal flat tubes taking into account five input variables: tube flattening (H), inlet volumetric flow rate (Q_i), wall heat flux (q_n^w), nanoparticle volume fraction ($\emptyset$) and nanoparticle diameter (d_p). The required output data to train the ANN was taken from the CFD simulation results which were performed using two phase mixture model. The predicted (Δp) by ANN was compared with the CFD simulated one and excellent agreement was observed. To view the accuracy of ANN model, statistical measures R^2, RMSE and MAPE were used and it was seen that the GMDH model has high accuracy in predicting the Δp values.

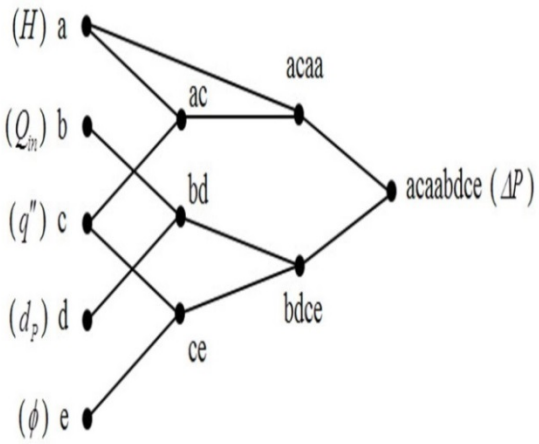


Fig.7. Evolved structure of generalized GMDH neural network for .

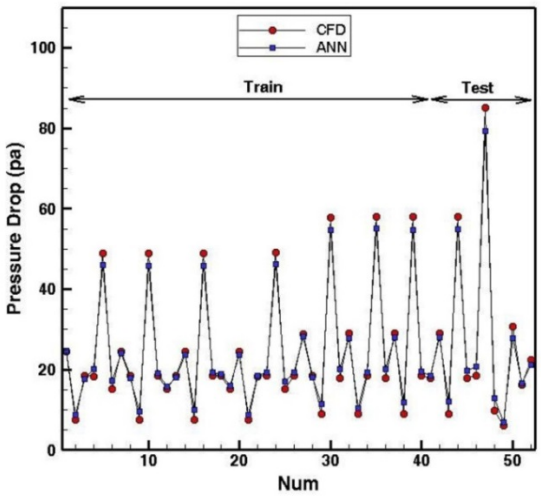


Fig. 8. Comparison of predicted by ANN and simulated by CFD.

Table.3.
Samples of numerical results using CFD

Num	Input Data					Output Data
	$H\,(mm)$	$Q_{in}\,(m^3/hr)$	$q''\,(kW/m^2)$	$\phi(\%)$	$d_P\,(nm)$	ΔP (pa)
1	4	0.005652	2	1.25	40	24.421
2	8	0.011304	2	1.25	40	15.098
3	8	0.011304	2	3.75	80	17.915
4	4	0.005652	4	1.25	80	24.519
5	6	0.008478	3	0	-	16.160
6	6	0.008478	3	2.5	100	18.441
7	6	0.008478	3	5	60	22.444
8	6	0.008478	3	2.5	60	18.404
9	4	0.005652	2	1.25	80	24.470
10	10	0.008478	3	2.5	60	7.5644
…						
52	2	0.008478	3	2.5	60	85.204

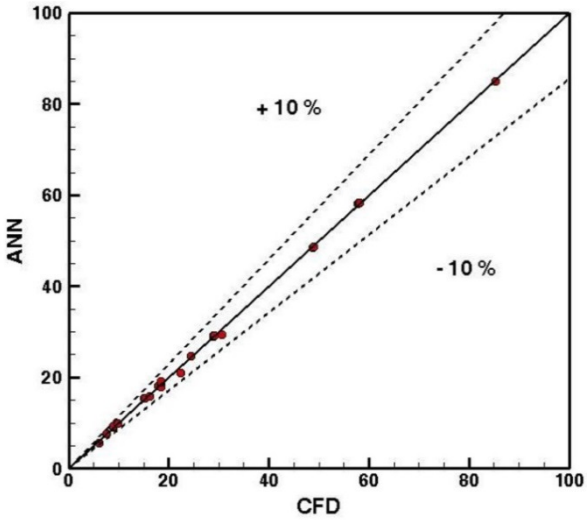


Fig.9. Comparison of predicted by ANN and simulated by CFD

References

[1] S.K. Das, N. Putra, P.W. Thiesen, R. Roetzel, Temperature dependence of thermal conductivity enhancement for nanofluids, J. Heat Transfer, 125 (2003) 567-574.

[2] S.M.S. Murshed, K.C. Leong, C. Yang, A combined model for the effective thermal conductivity of nanofluids, Appl. Thermal Eng. 29 (2009) 2477-2483.

[3] T.P. Teng, Y.H. Hung, T.C. Teng, H.E. Mo, H.G. Hsu, The effect of alumina/water nanofluid particle size on thermal conductivity, Appl. Thermal Eng. 30 (2010) 2213-2218.

[4] E. Ebrahimnia-Bajestan, H. Niazmand, W. Duangthongsuk, S. Wongwises, Numerical investigation of effective parameters in convective heat transfer of nanofluids flowing under a laminar flow regime, Int. J. Heat Mass Transfer 54 (2011) 4376–4388.

[5] M. Kalteh, A. Abbassi, M. Saffar-Avval, J. Harting, Eulerian–Eulerian two-phase numerical simulation of nanofluid laminar forced convection in a microchannel, Int. J. Heat Fluid Flow 32 (2011) 107–116 .

[6] R. Lotfi, Y. Saboohi, A.M. Rashidi, Numerical study of forced convective heat transfer of Nanofluids: Comparison of different approaches, Int. Commun. Heat Mass Transfer 37 (2010) 74–78.

[7] M. Shariat, A. Akbarinia, A. Hossein Nezhad, A. Behzadmehr, R. Laur, Numerical study of two phase laminar mixed convection nanofluid in elliptic ducts, Appl. Therm. Eng. 31 (2011) 2348-2359.

[8] P. Razi, M.A. Akhavan-Behabadi, M. Saeedinia, Pressure drop and thermal characteristics of CuO–base oil nanofluid laminar flow in flattened tubes under constant heat flux, Int. Commun. Heat Mass Transfer 38 (2011) 964–971.

[9] R.S. Vajjha, D.K. Das, P.K. Namburu, Numerical study of fluid dynamic and heat transfer performance of Al2O3 and CuO nanofluids in the flat tubes of a radiator, Int. J. Heat Fluid Flow 31 (2010) 613–621.

[10] S.J. Farlow, Self-organizing Method in Modeling: GMDH type algorithm. Marcel Dekker Inc, 1984.

[11] N. Nariman-Zadeh, A. Darvizeh, R. Ahmad-Zadeh, Hybrid genetic design of GMDH-type neural networks using singular value decomposition for modeling and prediction of the explosive cutting process, J. Eng. Manufact. 217 (2003) 779–790.

[12] N. Amanifard, N. Nariman-Zadeh, M.H. Farahani, A. Khalkhali, Modeling of multiple short-length-scale stall cells in an axial compressor using evolved GMDH neural networks, Energy Convers. Manag. 49 (2008) 2588–2594.

[13] H. Safikhani, M.A. Akhavan-Behabadi, N. Nariman-Zadeh, M.J. Mahmoodabadi, Modeling and multi-objective optimization of square cyclones using CFD and neural networks, Chemical Eng. Research Design 89 (2011) 301–309.

[14] M.J. Wilson, T.A. Newell, J.C. Chato, C.A.I. Ferreira, Refrigerant charge, pressure drop and condensation heat transfer in flattened tubes, Int. J. Refrig. 26 (2003) 442–451.

[15] J. Quiben, L. Cheng, J. Da Silva, J. R. Thome, Flow boiling in horizontal flattened tubes: Part I – Two-phase frictional pressure drop results and model, Int. J. Heat Mass Transfer 52 (2009) 3645–3653.

[16] M. Nasr, M. A. Akhavan-Behabadi, S. E. Marashi, Performance evaluation of flattened tube in boiling heat transfer enhancement and its effect on pressure drop, Int. Commun. Heat Mass Transfer 37 (2010) 430–436 .

[17] M. Manninen, V. Taivassalo, S. Kallio, On the mixture model for multiphase flow. VTT Publications, 1996.

[18] L. Schiller, A. Naumann, A drag coefficient correlation. Z. Ver Deutsch Ing, 1935 .

[19] B. Pak, Y. Cho, Hydrodynamic and heat transfer study of dispersed fluids with submicron metallic oxide particles, Exp. Heat Transfer 11 (1998) 151–170.

[20] Y. Xuan, W. Roetzel, Conceptions for heat transfer correlation of nanofluids, Int. J. Heat Mass Transfer 43 (2000) 3701–3707.

[21] N. Masoumi, N. Sohrabi, A. Behzadmehr, A new model for calculating the effective viscosity of nanofluids, J. Appl. Physics 42 (2009) 055501 (6 .(

[22] C. H. Chon,K. D. Kihm, S. P. Lee, S. U. S. Choi, Empirical correlation finding the role of temperature and particle size for nanofluid (Al2O3) thermal conductivity Enhancement, J. Appl. Physics 87 (2005) 153107 (3).

[23] K. Khanafer, K. Vafai, M. Lightstone, Buoyancy driven heat transfer enhancement in a two dimensional enclosure utilizing nanofluids, Int. J. Heat Mass Transfer 46 (2003) 3639-3653.

[24] A. Bejan, Convective heat transfer. John Wiley & Sons Inc, 2004.

[25] S. V. Patankar, Numerical Heat Transfer Fluid Flow. Washington: Hemisphere, 1980 .

[26] R. K. Shah, A. L. London, Laminar Flow Forced Convection in Ducts. New York: Academic Press, 1978 .

[27] S. Mirmasoumi, A. Behzadmehr, Effect of nanoparticles mean diameter on mixed convection heat transfer of a nanofluid in a horizontal tube, Int. J. Heat Fluid Flow 29 (2008) 557-566 .

[28] A. G. Ivakhnenko, Polynomial theory of complex systems. IEEE Trans Sys Man Cybern. SMC-1, 1971.

[29] C. Douglas Montgomery, Design and Analysis Experiments. John Wiley & Son Inc, 1991.

[30] T. H. Hou, C. H. Su, W. L. Liu, Parameters optimization of a nano-particle wet milling process using the Taguchi method, response surface method and genetic algorithm, Powder Technolog. 173 (2007) 153–162.